*Bulletin of Mathematical Biology*, Vol. 42, pp. 461–480
Pergamon Press Ltd. 1980. Printed in Great Britain

0007-4985/80/0501-0461 $02.00/0

# MODELS OF HUMAN LUNG AIRWAYS AND THEIR APPLICATION TO INHALED PARTICLE DEPOSITION

HSU-CHI YEH and G. M. SCHUM†
Inhalation Toxicology Research Institute,
Lovelace Biomedical and Environmental Research Institute,
P.O. Box 5890, Albuquerque, NM 87115

Models of the human respiratory tract were developed based on detailed morphometric measurements of a silicone rubber cast of the human tracheobronchial airways. Emphasis was placed on the "Typical Path Lung Model" which used one typical pathway to represent a portion of the lung, such as a lobe, or to represent the whole lung. The models contain geometrical parameters, including airway segment diameters, lengths, branching angles and angles of inclination to gravity, which are needed for estimating inhaled particle deposition. Aerosol depositions for various breathing patterns and particle sizes were calculated using these lung models and the modified Findeisen–Landahl computational scheme. The results agree reasonably well with recent experimental data. Regional deposition, including lobar deposition fractions, are also calculated and compared with results based on the ICRP lung deposition model.

*1. Introduction.* Knowledge of initial deposition pattern of inhaled particles is of interest in toxicology studies using laboratory animals and in assessing hazards to people from airborne toxicants present in the environment. One approach to understanding the deposition of inhaled particles is the use of mathematical models.

The geometry of the tracheobronchial airways is one of the factors influencing particle deposition during inhalation. Airway structure parameters which influence particle deposition include airway segment diameters, lengths, branching angles and angles of inclination to gravity (Yeh *et al.*, 1976). Because of the complexity of lung anatomy and the mathematical calculations involved in particle deposition, most of the lung models have had fairly simple simulated lung structures (Davies, 1961; Findeisen, 1935; Horsfield *et al.*, 1971; Landahl, 1950; Olson *et al.*, 1970;

†Present address: Department of Biology, San Diego State University, San Diego, CA, U.S.A.

Weibel, 1963). Various deposition models have been developed based on these lung models (Beeckmans, 1965a,b; Findeisen, 1935; Landahl, 1950; Task Group on Lung Dynamics, 1966; Taulbee and Yu, 1975). Values of some of the geometric parameters such as branching angles and gravity angles were assumed, since those lung models supplied only part of the needed information (mainly airway segment diameters and lengths). Furthermore, laboratory animals are usually used in inhalation toxicological studies in place of human subjects. Lack of appropriate lung models causes difficulties in predicting particle deposition in each species and hinders the extrapolation of animal data to man. One of our goals in lung modeling studies is to develop a modeling method which could be applied not only to humans but also to various mammalian species commonly used in laboratory inhalation studies. This paper describes two models of the human tracheobronchial airways, developed with the same principles and techniques used in our laboratory for developing lung models for various mammalian species (Yeh *et al.*, 1979). The modified Findeisen–Landahl deposition model was applied to these newly developed lung models to calculate aerosol deposition for various breathing patterns and particle sizes.

*2. Material and Methods.* A silicone rubber replica cast of human tracheobronchial airways was carefully prepared and measured to provide the basic data on the geometry of lung airways. To provide accurate orientation of the airway segments, the cast was made in a lung that was intact and still within the thorax using a method described by Phalen *et al.* (1973). After the injected silicone rubber had cured *in situ*, the lung was removed from the thorax and the tissues were digested with sodium hydroxide. The flexible replica was trimmed to the level of the terminal bronchiole before being subjected to detailed measurements (Phalen *et al.*, 1978).

The trimmed cast was used to obtain airway segment diameters, lengths, branching angles and angles of inclination to gravity. To provide a basis for morphometric measurements and to assure proper linkage of the airway segments, an idealized model of an airway branch and a unique binary identification scheme were used (Phalen *et al.*, 1978). One human lung cast was selected. The lung cast was obtained from a 60 year old and about 80 kg in weight male subject who died of a myocardial infarction. No abnormalities in the lung were observed in lung sections. Every airway segment with diameter $\geqq 3$ mm and about 20% of the rest randomly selected were measured from the trimmed cast to the nearest 0.1 mm for lengths and diameters and 5° for angles. A report detailing all these raw

data has been published as Lovelace Foundation Document Number LF-53 (March, 1976), *Tracheobronchial Geometry: Human, Dog, Rat, Hamster.* Measurement errors were estimated to be less than 10% in length and diameter and 10° for angles (Phalen *et al.*, 1978). Details of the casting technique, measuring scheme and evaluation of the casts were reported elsewhere (Phalen *et al.*, 1973, 1978; Yeh *et al.*, 1975).

*3. Lung Models.* A fairly simple anatomical lung model is desirable for most applications. In our modeling concept, we try to use $n$ number of identical pathways to represent $n$ number of actual (or estimated) pathways of a complicated tree structure, such as each lobe of a lung or a whole lung. We termed this type of lung model a "Typical Path Lung Model". This concept is essentially the same as Weibel's Model A lung model, except that it does not require the tree structure to be symmetrical and it is also applicable to model a portion of the lung, such as a lobe. A computer program was written to trace all available pathways from the trachea down to each terminal bronchiole. The numbers of pathways terminating at various generations (trachea = generation 1) were counted to form a frequency distribution. From this distribution, the median generation number was obtained. Table I lists the median generation number, $N_m$, and the observed range of generations where pathways terminated for each lung lobe. Mean or median values of geometrical parameters, such as airway segment diameters, lengths, branching angles and gravity angles were obtained by tracing all pathways terminating at $N_m$ in the portion of

TABLE I

Range and Median Generation Number Between Trachea and Terminal Bronchioles and Calculated Values of $X$ (Average Branching Ratio in the Model) with Estimated Number of Terminal Bronchioles, $N_t$

| Lobe | Generation number between trachea and terminal bronchioles | | Estimated $N_t$ | $X$ |
|---|---|---|---|---|
| | Range | Median | | |
| Right upper | 9–20 | 15 | 2938 | 1.95 |
| Right middle | 10–20 | 15 | 2375 | 2.03 |
| Right lower | 12–22 | 17 | 8455 | 2.00 |
| Left upper | 11–22 | 15 | 2958 | 1.95 |
| Left lower | 13–22 | 16 | 9723 | 2.03 |
| Whole lung | 9–22 | 16 | 26449 | 1.97 |

the lung involved. The number of segments in each generation in the model, which has $N_m$ generations between trachea and terminal bronchioles, was calculated from the following formula (Yeh, 1980).

$$N_n = X^{n-I}, \tag{1}$$

where $N_n$ is the number of segments in $n$th generation, $I$ is the generation number of the main stem segment. The value of $X$, which is equivalent to average branching ratio in the model, depends on the branching pattern of the tree structure and can be calculated if both the number of terminal bronchioles and the median generation number for terminal bronchioles are known or can be reasonably estimated from morphometric data. The values of $X$ and the estimated number of terminal bronchioles are also listed in Table I. The values of $X$ for different lung lobes are very close to 2 with an average value of 1.99. Because the sampling scheme used in morphometric measurements caused some uncertainty in estimated number of terminal bronchioles, and also for the sake of simplicity, $X=2$ was used in all lobes in this study. The model was extended to include several generations of respiratory bronchioles, alveolar ducts, sacs and alveoli, assuming total number of alveoli of $3\times10^8$ (Weibel, 1963) and a total lung capacity of 5600 $cm^3$ for a standard size man (ICRP, 1974). In the pulmonary region, random orientation for both branching angles (0 to 90° in two dimensions) and gravity angles (0 to 90° in three dimensions) were assumed. Hence, 45° for the branching angle and 60° for the gravity angle (90° corresponding to a horizontal tube) were obtained. The detailed modeling method applied in this study has been described by Yeh *et al.* (1979). The results of the models are presented in Table II for the whole lung model and in Appendix A (Tables AI–AV) for the lobar models with each table representing a lobe. The dimensions listed in these tables are believed to correspond to a lung inflated to the total lung capacity (TLC) because of the pressure of 0.5–1.0 psig used in injecting casting material. Therefore, for practical applications, the airway dimensions should be scaled down to lung volumes of interest. A comparison of lobar lung volumes, anatomical dead spaces, and relative lobar size are given in Appendix A (Tables AVI–AVII) for different models and data. The agreement is satisfactory. Brief comparisons between the various models are given in Table III.

*4. Theoretical Estimation of Particle Deposition.* Simplified models of lung airway structure and of air flow patterns are desired for theoretical estimations of particle deposition. Although many important experimental

TABLE II

Typical Path Lung Model: Human—Whole Lung

| $n$ | Number of tubes | $L$ (cm) | $d$ (cm) | $\Theta$ (°) | $\Phi$ (°) | $S$ (cm$^2$) | $V$ (cm$^3$) | $\Sigma V$ (cm$^3$) |
|---|---|---|---|---|---|---|---|---|
| 1 | 1 | 10.0 | 2.01 | 0 | 0 | 3.17 | 31.73 | 31.73 |
| 2 | 2 | 4.36 | 1.56 | 33 | 20 | 3.82 | 16.67 | 48.40 |
| 3 | 4 | 1.78 | 1.13 | 34 | 31 | 4.01 | 7.14 | 55.54 |
| 4 | 8 | 0.965 | 0.827 | 22 | 43 | 4.30 | 4.15 | 59.69 |
| 5 | 16 | 0.995 | 0.651 | 20 | 39 | 5.33 | 5.30 | 64.98 |
| 6 | 32 | 1.01 | 0.574 | 18 | 39 | 8.28 | 8.36 | 73.35 |
| 7 | 64 | 0.890 | 0.435 | 19 | 40 | 9.51 | 8.47 | 81.81 |
| 8 | 128 | 0.962 | 0.373 | 22 | 36 | 13.99 | 13.46 | 95.27 |
| 9 | 256 | 0.867 | 0.322 | 28 | 39 | 20.85 | 18.07 | 113.34 |
| 10 | 512 | 0.667 | 0.257 | 22 | 45 | 26.56 | 17.72 | 131.06 |
| 11 | 1024 | 0.556 | 0.198 | 33 | 43 | 31.53 | 17.53 | 148.59 |
| 12 | 2048 | 0.446 | 0.156 | 34 | 45 | 39.14 | 17.46 | 166.05 |
| 13 | 4096 | 0.359 | 0.118 | 37 | 45 | 44.79 | 16.08 | 182.13 |
| 14 | 8192 | 0.275 | 0.092 | 39 | 60 | 54.46 | 14.98 | 197.10 |
| 15 | 16,384 | 0.212 | 0.073 | 39 | 60 | 68.57 | 14.54 | 211.64 |
| 16† | 32,768 | 0.168 | 0.060 | 51 | 60 | 92.65 | 15.57 | 227.21 |
| 17 | 65,536 | 0.134 | 0.054 | 45 | 60 | 150.09 | 20.11 | 247.32 |
| 18 | 131,072 | 0.120 | 0.050 | 45 | 60 | 257.36 | 30.88 | 278.20 |
| 19 | 262,144 | 0.092 | 0.047 | 45 | 60 | 454.81 | 41.84 | 320.04 |
| 20 | 524,288 | 0.080 | 0.045 | 45 | 60 | 833.84 | 66.71 | 386.75 |
| 21 | 1,048,576 | 0.070 | 0.044 | 45 | 60 | 1,594.39 | 111.61 | 498.36 |
| 22 | 2,097,152 | 0.063 | 0.044 | 45 | 60 | 3,188.78 | 200.89 | 699.25 |
| 23 | 4,194,304 | 0.057 | 0.043 | 45 | 60 | 6,090.97 | 347.19 | 1,046.44 |
| 24 | 8,388,608 | 0.053 | 0.043 | 45 | 60 | 12,181.95 | 645.64 | 1,692.08 |
| 25‡ | $3 \times 10^8$ | 0.025 | 0.030 | 45 | 60 | — | 3,871.80 | 5,563.88 |

†Terminal bronchioles.

‡Alveoli.

$n$ = generation number; $L$ = airway segment length; $d$ = segment diameter; $\Theta$ = branching angle; $\Phi$ = gravity angle with 90° corresponding to a horizontal tube; $S$ = cross-sectional area; $V$ = volume; $\Sigma V$ = cumulative volume.

studies of particle deposition in the human respiratory tract have been made (Lippmann, 1977; Mercer, 1975), the theoretical calculations have the advantage that they can be readily applied to any breathing pattern, particle size or particle density.

Because of the extreme complexity of the structures in the nasopharyngeal region, empirical equations are often used for calculating nasopharyngeal deposition. The equation used in this study was the one suggested by the Task Group on Lung Dynamics (1966) which can be written as

$$N = -0.62 + 0.475 \log (D_a^2 F), \tag{2}$$

## TABLE III
## Comparison of Human Lung Models

| Model | Terminal bronchioles | | | | Right:left | Branching/gravity angles |
|---|---|---|---|---|---|---|
| | Generation number† | $N_t$ | $d$ (mm) | $L$ (mm) | | |
| Present lobar model | 15–17 | 26,624 | 0.51–0.66 | 1.18–2.15 | 54:46 | available |
| Present whole lung model | 16 | 32,768 | 0.6 | 1.68 | — | available |
| Horsfield model Model 1 (1971) | — | 29,240 | 0.48 | 1.05 | 55:45 | indirect/NA |
| Horsfield (1968) | — | 27,993 | 0.6 | — | — | NA |
| Weibel (1963) | 17 | 65,536 | 0.6 | 1.65 | — | NA |
| Landahl (1950) | 8 | 60,000 | 0.6 | 3.0 | — | NA |
| Findeison (1935) | 6 | 54,000 | 0.6 | 3.0 | — | NA |

†Trachea = generation 1.
$N_t$ = number of terminal bronchioles; $d$ = diameter; $L$ = length, $NA$ = not available.

where $N$ is the fraction of particles with aerodynamic diameter $D_a$ (in $\mu$m) which is deposited in the nose and $F$ (l/min) is the inspiratory flow rate. The total deposition in the nasopharyngeal region, NP, is given by

$$\mathrm{NP} = N_i + N_e(1 - N_i)[1 - (\mathrm{TB}' + \mathrm{P}')(1 - V_n/V_t)] \tag{3}$$

where $N_i$ and $N_e$ are obtained from equation (2) for inhalation and exhalation, respectively, TB′ and P′ represent the fractional deposition in the tracheobronchial and pulmonary regions, respectively, relative to the number of particles entering the trachea, $V_n$ is the volume of the nasopharyngeal region and $V_t$ is the tidal volume. In this study, we assumed that $V_n$ was equal to $50\,\mathrm{cm}^3$, that there was no pause between inhalation and exhalation and that $N_i = N_e = N$. The deposition in tracheobronchial (TB) and pulmonary (P) regions become

$$\mathrm{TB} = (1 - N)(1 - V_n/V_t)\mathrm{TB}' \tag{4a}$$

$$\mathrm{P} = (1 - N)(1 - V_n/V_t)\mathrm{P}' \tag{4b}$$

To permit comparisons with mouth breathing experimental data, theoretical values for TB and P are adjusted by

$$\mathrm{TB\ or\ P\ (mouth\ breathing)} = [\mathrm{TB\ or\ P\ (nasal\ breathing)}]/[1 - N] \tag{5}$$

and the sum of TB and P becomes total deposition due to mouth breathing. One notes that with this approximation, the amount deposited in the mouth region is not taken into account.

To calculate TB′ and P′, the lung model described in the previous section was used along with the method of calculation similar to Findeisen (1935) and Landahl (1950). Briefly, we first adjusted airway dimensions to equal normal lung volume, i.e. functional residual capacity (FRC) plus one half of tidal volume (TV), assuming (1) FRC = 0.6 TLC, (2) conducting airway diameters expand as square root of volume expansion and (3) both diameters and lengths in respiratory region are proportional to the cube root of the lung volume (Schum and Yeh, 1979). Fraction of aerosol deposited on each generation was calculated, using deposition equations due to inertial impaction, sedimentation and diffusion as listed in Table IV (Schum and Yeh, 1979). Adjustments were made in the calculations to compensate for deposition in previous generations and for the fraction of tidal air not penetrating to the generation in consideration. For a given

## TABLE IV
## Deposition Equations

A. *Deposition by Diffusion*

For laminar flow

$$P_D = 1 - 0.819\,e^{-7.315x} - 0.0976\,e^{-44.61x} - 0.0325\,e^{-114x} - 0.0509\,e^{-79.31x^{2/3}} \quad (1)$$

where

$$x = \frac{LD}{2R^2\bar{v}}$$

$P_D$ = diffusion deposition probability
$D$ = diffusion coefficient of particles
$R$ = radius of tube or airway
$\bar{v}$ = mean flow velocity
$L$ = length of tube or airway segment.

For turbulent flow

$$P_D = \frac{2\sqrt{Dt}}{R}\left(1 - \frac{2\sqrt{Dt}}{9R} + \ldots\right) = 2.828x^{1/2}(1 - 0.314x^{1/2} + \ldots) \quad (2)$$

where

$t$ = time for flow to pass through the tube or airway segment = $L/\bar{v}$.

For a pause

$$P_D^p = 1 - \exp(-5.784KTCt/6\pi\mu r_p R^2) \quad (3)$$

where $t$ is the pause time, $K$ is Boltzmann constant, $T$ is the temperature in K, $C$ is the Cunningham slip correction factor, $r_p$ is the radius of the particle, $\mu$ is the viscosity of fluid and the superscript $p$ in $P_D^p$ stands for pause.

B. *Deposition by Sedimentation*

$$P_s = 1 - \exp\left[\frac{-4gC\rho_p r_p^2 L\cos\phi}{9\pi\mu R\bar{v}}\right] \quad (4)$$

where

$P_s$ = sedimentation deposition probability
$\rho_p$ = density of the particle
$\phi$ = inclination angle relative to gravity ($\phi = 0°$ for horizontal tube).

For a pause, $L/\bar{v}$ is replaced by $t$ (the pause time) in equation (4).

C. *Deposition by Inertial Impaction*

$$P_I = 1 - \frac{2}{\pi}\cos^{-1}(\theta \cdot St) + \frac{1}{\pi}\sin\{2\cos^{-1}(\theta \cdot St)\} \quad \text{for} \quad \theta \cdot St < 1 \quad (5)$$

$$P_I = 1 \quad \text{for} \quad \theta \cdot St \geqq 1$$

where

$P_I$ = impaction deposition probability
$\theta$ = bend angle or branching angle (in radians)
$St$ = Stokes' number = $\dfrac{C\rho_p r_p^2 \bar{v}}{9\mu R}$.

breathing frequency, equal time was allocated for inspiration and expiration with no pause in between. Lobar depositions were also calculated by assuming that the flow distribution to each lobe was proportional to the number of terminal bronchioles (or alveoli) associated with each lobe. The deposition fractions were also adjusted for the amount deposited in the common stem segments such as the trachea, right or left lung main bronchi which were not belonging to any particular lobe. Details of the method of calculation applied in this study have been described by Schum and Yeh (1979).

Table V shows the results of the calculations for tidal volumes of 750 $cm^3$, 1450 $cm^3$ and 2150 $cm^3$ with breathing frequency of 15 breath/min

TABLE V
Calculated Deposition of Unit Density Spheres†

| Tidal volume | Region | Particle diameter, $\mu m$ | | | | | | | | | |
|---|---|---|---|---|---|---|---|---|---|---|---|
| | | 0.01 | 0.06 | 0.20 | 0.60 | 1.0 | 2.0 | 3.0 | 4.0 | 6.0 | 10.0 |
| 750 $cm^3$ | NP | 0 | 0 | 0 | 0 | 0.041 | 0.454 | 0.607 | 0.694 | 0.816 | 0.978 |
| | TB | 0.472 | 0.098 | 0.033 | 0.019 | 0.023 | 0.039 | 0.055 | 0.068 | 0.073 | 0.016 |
| | P | 0.298 | 0.344 | 0.148 | 0.092 | 0.118 | 0.178 | 0.193 | 0.170 | 0.094 | 0.006 |
| 1450 $cm^3$ | NP | 0 | 0 | 0 | 0 | 0.267 | 0.594 | 0.712 | 0.791 | 0.917 | |
| | TB | 0.395 | 0.073 | 0.025 | 0.016 | 0.018 | 0.031 | 0.043 | 0.048 | 0.035 | |
| | P | 0.465 | 0.459 | 0.196 | 0.126 | 0.141 | 0.195 | 0.189 | 0.145 | 0.049 | |
| 2150 $cm^3$ | NP | 0 | 0 | 0 | 0.053 | 0.388 | 0.674 | 0.779 | 0.854 | 0.982 | |
| | TB | 0.345 | 0.060 | 0.021 | 0.014 | 0.017 | 0.030 | 0.039 | 0.039 | 0.005 | |
| | P | 0.550 | 0.477 | 0.199 | 0.126 | 0.133 | 0.172 | 0.153 | 0.103 | 0.013 | |

†For 15 breaths per minute with no pause and FRC = 0.4 TLC.
NP = nasopharyngeal: TB = tracheobronchial; P = pulmonary.

for unit density spheres. When compared with the results of the Task Group model (Table 1 in Task Group on Lung Dynamics, 1966), one observes that the Task Group model predicts higher pulmonary deposition than the present model in almost every case. It has been shown that the Task Group model overestimates the pulmonary deposition when compared with the best available experimental data on normal human beings (Lippmann, 1977). Comparison between the present results and available experimental data is shown in Figures 1–3. Figure 1 shows the total deposition during nasal breathing for tidal volumes of 750 $cm^3$ and 1450 $cm^3$ with 15 breath/min and the data of Giacomelli-Maltoni *et al.* (1972) and Heyder *et al.* (1975). The agreement is satisfactory. In Figures 2

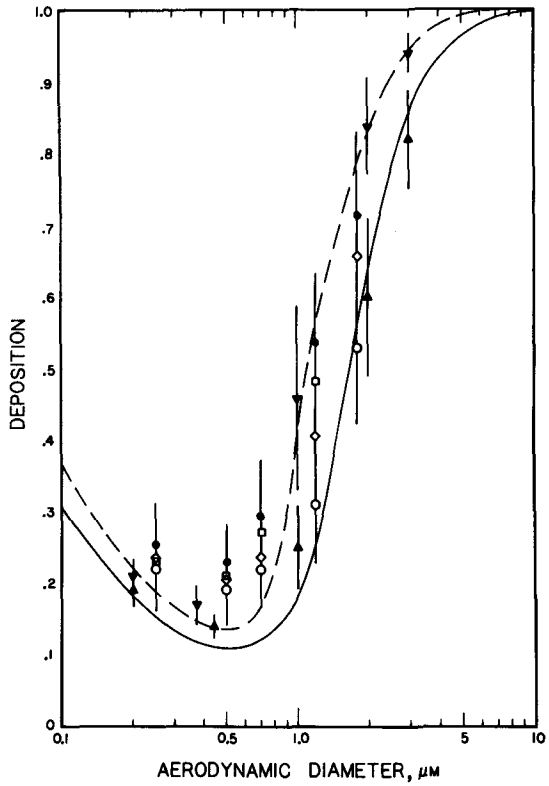


Figure 1. Total deposition during nasal breathing. ● Giacomelli-Maltoni *et al.* (1972). 12 breath/min, 1000 $cm^3$ tidal volume; □Giacomelli-Maltoni *et al.* (1972), 8–19 breath/min, 400–1500 $cm^3$ tidal volume; ○ Giacomelli-Maltoni *et al.* (1972), 12 breath/min, 750 $cm^3$ tidal volume; ◇ Giacomelli-Maltoni *et al.* (1972), 12 breath/min, 1500 $cm^3$ tidal volume; ▲ Heyder *et al.* (1975), 500 $cm^3$ tidal volume; ▼ Heyder *et al.* (1975), 1000 $cm^3$ tidal volume. Curves: present model —— 750 $cm^3$ tidal volume, – – – 1450 $cm^3$ tidal volume with 15 breath/min and unit density spheres

and 3, the experimental results obtained by various investigators for mouth breathing for a variety of respiratory frequencies and tidal volumes in human subjects are compared with the calculated deposition of particles entering the trachea [equation (5)]. The agreements are fairly good despite the fact that the calculated values do not take into account the amount of particles deposited in the mouth region, including possible loss in the mouthpiece. It has been shown that the deposition in the mouth region, M, increases as particle size increases for a given inspiratory flow rate (Task Group on Lung Dynamics, 1966). If an empirical equation for mouth deposition as a function of particle size, flow rate and other parameters could be established, then it would be expected that when the correction

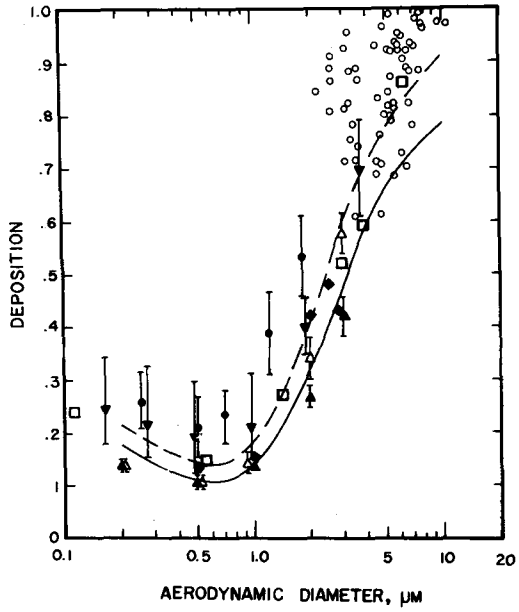


Figure 2. Total deposition during mouth breathing. ● Giacomelli-Maltoni *et al.* (1972); ○ Lippmann (1977); □ Landahl (1951); ▼ Altshuler *et al.* (1967); ◆ Lever (1973); ▲ Heyder *et al.* (1975), 500 $cm^3$ tidal volume; △ Heyder *et al.* (1975), 1000 $cm^3$ tidal volume. Curves: present model —— 750 $cm^3$ tidal volume, – – – 1450 $cm^3$ tidal volume with 15 breath/min and unit density spheres

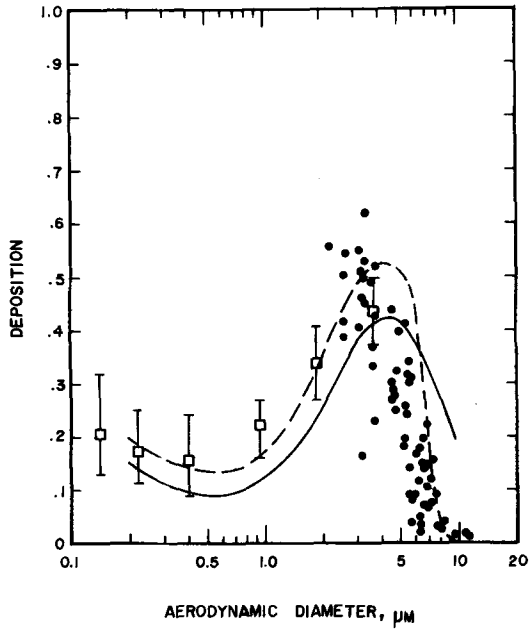


Figure 3. Pulmonary deposition during mouth breathing. ● Lippmann (1977); □ Altshuler *et al.* (1967). Curves: present model —— 750 $cm^3$ tidal volume, – – – 1450 $cm^3$ tidal volume with 15 breath/min and unit density spheres

was made for mouth deposition, the agreement between the calculated values and data would be improved. Unfortunately no such empirical equation for mouth deposition is available at the present time, due to lack of such data. The results of lobar deposition calculation for 750 $cm^3$ tidal volume with 15 breath/min are shown in Table VI. Also included in this table are the results calculated for the whole lung model. The agreement

TABLE VI

Calculated Lobar Deposition of Unit Density Spheres†

| $d_p$, μm | Region | R.U. | R.M. | R.L. | L.U. | L.L. | C. stem | Sum | W.L. |
|---|---|---|---|---|---|---|---|---|---|
| 0.01 | NP | — | — | — | — | — | — | 0 | 0 |
| | TB | 0.0603 | 0.0279 | 0.123 | 0.0656 | 0.129 | 0.0321 | 0.438 | 0.472 |
| | P | 0.0539 | 0.0288 | 0.0985 | 0.0453 | 0.0925 | — | 0.319 | 0.298 |
| 0.06 | NP | — | — | — | — | — | — | 0 | 0 |
| | TB | 0.0119 | 0.0053 | 0.0243 | 0.0133 | 0.0260 | 0.0072 | 0.0880 | 0.0976 |
| | P | 0.0566 | 0.0298 | 0.101 | 0.0503 | 0.0990 | — | 0.337 | 0.344 |
| 0.2 | NP | — | — | — | — | — | — | 0 | 0 |
| | TB | 0.0041 | 0.0018 | 0.0079 | 0.0043 | 0.0085 | 0.0029 | 0.0295 | 0.0328 |
| | P | 0.0243 | 0.0128 | 0.0423 | 0.0214 | 0.0417 | — | 0.143 | 0.148 |
| 0.6 | NP | — | — | — | — | — | — | 0 | 0 |
| | TB | 0.0024 | 0.0011 | 0.0047 | 0.0025 | 0.0051 | 0.0016 | 0.0174 | 0.0188 |
| | P | 0.0150 | 0.0079 | 0.0264 | 0.0133 | 0.0259 | — | 0.0885 | 0.0922 |
| 1.0 | NP | — | — | — | — | — | — | 0.041 | 0.041 |
| | TB | 0.0032 | 0.0014 | 0.0062 | 0.0033 | 0.0068 | 0.0014 | 0.0222 | 0.0232 |
| | P | 0.0191 | 0.0101 | 0.0340 | 0.0169 | 0.0332 | — | 0.113 | 0.117 |
| 2.0 | NP | — | — | — | — | — | — | 0.454 | 0.454 |
| | TB | 0.0056 | 0.0025 | 0.0112 | 0.0057 | 0.0121 | 0.0015 | 0.0386 | 0.0393 |
| | P | 0.0285 | 0.0150 | 0.0517 | 0.0257 | 0.0502 | — | 0.171 | 0.178 |
| 3.0 | NP | — | — | — | — | — | — | 0.607 | 0.607 |
| | TB | 0.0079 | 0.0037 | 0.0161 | 0.0080 | 0.0174 | 0.0020 | 0.0551 | 0.0553 |
| | P | 0.0309 | 0.0163 | 0.0566 | 0.0283 | 0.0550 | — | 0.187 | 0.193 |
| 4.0 | NP | — | — | — | — | — | — | 0.694 | 0.694 |
| | TB | 0.0096 | 0.0045 | 0.0198 | 0.0097 | 0.0211 | 0.0026 | 0.0673 | 0.0676 |
| | P | 0.0271 | 0.0142 | 0.0502 | 0.0251 | 0.0485 | — | 0.165 | 0.170 |
| 6.0 | NP | — | — | — | — | — | — | 0.816 | 0.816 |
| | TB | 0.0106 | 0.0050 | 0.0217 | 0.0105 | 0.0229 | 0.0031 | 0.0738 | 0.0732 |
| | P | 0.0150 | 0.0078 | 0.0278 | 0.0140 | 0.0264 | — | 0.0910 | 0.0935 |
| 10.0 | NP | — | — | — | — | — | — | 0.978 | 0.978 |
| | TB | 0.0024 | 0.0012 | 0.0048 | 0.0023 | 0.0050 | 0.0010 | 0.0167 | 0.0165 |
| | P | 0.0009 | 0.0005 | 0.0016 | 0.0008 | 0.0015 | — | 0.0053 | 0.0056 |

†For tidal volume = 750 $cm^3$, 15 breaths per minute with no pause and FRC = 0.4 TLC.

NP = nasopharyngeal; TB = tracheobronchial; P = pulmonary; RU = right upper lobe; RM = right middle lobe; RL = right lower lobe; LU = left upper lobe; LL = left lower lobe; WL = whole lung; C. stem = common stems.

between the whole lung and the lobar models is quite good and the differences are less than 10% for all cases studied here. Unfortunately no lobar deposition data of humans are available for comparison.

5. *Summary.* Lung models describing the morphometric dimension of the human lung airways have been developed based on detailed morphometric measurements on a replica cast of a human lung. Using a similar approach to the Findeisen–Landahl computational method, the lung models were applied to predict the deposition of airborne particles in different regions of the lung. The theoretical predictions for pulmonary depositions were generally lower than those predicted by the Task Group model. Available deposition data on nasal breathing and mouth breathing were compared with calculated values and the agreement between the predicted values and data was satisfactory.

Research supported by the National Institute of Environmental Health Sciences and U.S. Department of Energy under Contract Number EY-76-C-04-1013 and conducted in animal care facilities fully accredited by the American Association for Accreditation of Laboratory Animal Care.

The authors are grateful for the critical review of the manuscript by Drs R. G. Cuddihy, R. O. McClellan, J. L. Mauderly, M. B. Snipes and R. K. Wolff, to Drs O. G. Raabe and R. F. Phalen for their beneficial discussions and suggestions, to Mr Emerson E. Goff for preparing the illustrations and to Mrs Judy Miller for typing the manuscript.

# APPENDIX A

TABLE AI
Typical Path Lung Model: Human—Right Upper Lobe

| $n$ | Number of tubes | $L$ (cm) | $d$ (cm) | $\Theta$ (°) | $\Phi$ (°) | $S$ (cm$^2$) | $V$ (cm$^3$) | $\Sigma V$ (cm$^3$) |
|---|---|---|---|---|---|---|---|---|
| 1 | 1 | 10.0 | 2.01 | 0 | 0 | 3.17 | 31.73 | 31.73 |
| 2 | 1 | 3.09 | 1.75 | 25 | 25 | 2.41 | 7.43 | 39.16 |
| 3 | 1 | 1.22 | 1.02 | 60 | 60 | 0.82 | 1.00 | 40.16 |
| 4 | 2 | 0.800 | 0.760 | 28 | 63 | 0.91 | 0.73 | 40.89 |
| 5 | 4 | 1.27 | 0.650 | 30 | 60 | 1.33 | 1.69 | 42.57 |
| 6 | 8 | 1.25 | 0.579 | 17 | 58 | 2.11 | 2.63 | 45.20 |
| 7 | 16 | 0.827 | 0.454 | 22 | 68 | 2.59 | 2.14 | 47.35 |
| 8 | 32 | 0.988 | 0.355 | 31 | 51 | 3.17 | 3.13 | 50.48 |
| 9 | 64 | 0.798 | 0.278 | 37 | 52 | 3.88 | 3.10 | 53.58 |
| 10 | 128 | 0.557 | 0.216 | 38 | 47 | 4.69 | 2.61 | 56.19 |
| 11 | 256 | 0.401 | 0.158 | 43 | 45 | 5.02 | 2.01 | 58.20 |
| 12 | 512 | 0.350 | 0.118 | 46 | 45 | 5.60 | 1.96 | 60.16 |
| 13 | 1024 | 0.250 | 0.088 | 47 | 60 | 6.23 | 1.56 | 61.72 |
| 14 | 2048 | 0.194 | 0.070 | 48 | 60 | 7.88 | 1.53 | 63.25 |
| 15† | 4096 | 0.143 | 0.058 | 52 | 60 | 10.82 | 1.55 | 64.79 |
| 16 | 8192 | 0.119 | 0.053 | 45 | 60 | 18.07 | 2.15 | 66.94 |
| 17 | 16,384 | 0.102 | 0.049 | 45 | 60 | 30.90 | 3.15 | 70.09 |
| 18 | 32,768 | 0.089 | 0.047 | 45 | 60 | 56.85 | 5.06 | 75.15 |
| 19 | 65,536 | 0.078 | 0.045 | 45 | 60 | 104.23 | 8.13 | 83.28 |
| 20 | 131,072 | 0.070 | 0.044 | 45 | 60 | 199.30 | 13.95 | 97.23 |
| 21 | 262,144 | 0.063 | 0.044 | 45 | 60 | 398.60 | 25.11 | 122.34 |
| 22 | 524,288 | 0.057 | 0.043 | 45 | 60 | 761.37 | 43.40 | 165.74 |
| 23 | 1,048,576 | 0.053 | 0.043 | 45 | 60 | 1522.74 | 80.71 | 246.45 |
| 24‡ | $4.62 \times 10^7$ | 0.025 | 0.030 | 45 | 60 | — | 596.26 | 842.71 |

†Terminal bronchioles.
‡Alveoli.
$n$ = generation number; $L$ = airway segment length; $d$ = segment diameter; $\Theta$ = branching angle; $\Phi$ = gravity angle with 90° corresponding to a horizontal tube; $S$ = cross-sectional area; $V$ = volume; $\Sigma V$ = cumulative volume.

TABLE AII

Typical Path Lung Model: Human—Right Middle Lobe

| $n$ | Number of tubes | $L$ (cm) | $d$ (cm) | $\Theta$ (°) | $\Phi$ (°) | $S$ ($cm^2$) | $V$ ($cm^3$) | $\Sigma V$ ($cm^3$) |
|---|---|---|---|---|---|---|---|---|
| 1 | 1 | 10.0 | 2.01 | 0 | 0 | 3.17 | 31.73 | 31.73 |
| 2 | 1 | 3.09 | 1.75 | 25 | 25 | 2.41 | 7.43 | 39.16 |
| 3 | 1 | 3.02 | 1.33 | 15 | 5 | 1.39 | 4.20 | 43.36 |
| 4 | 1 | 2.27 | 0.720 | 25 | 35 | 0.41 | 0.92 | 44.28 |
| 5 | 2 | 1.34 | 0.620 | 18 | 35 | 0.60 | 0.81 | 45.09 |
| 6 | 4 | 1.63 | 0.528 | 28 | 33 | 0.88 | 1.43 | 46.52 |
| 7 | 8 | 1.04 | 0.376 | 18 | 30 | 0.89 | 0.92 | 47.44 |
| 8 | 16 | 1.04 | 0.317 | 31 | 31 | 1.26 | 1.31 | 48.76 |
| 9 | 32 | 0.691 | 0.268 | 38 | 32 | 1.81 | 1.25 | 50.00 |
| 10 | 64 | 0.527 | 0.199 | 45 | 49 | 1.99 | 1.05 | 51.05 |
| 11 | 128 | 0.394 | 0.147 | 50 | 45 | 2.17 | 0.86 | 51.91 |
| 12 | 256 | 0.266 | 0.106 | 52 | 45 | 2.26 | 0.60 | 52.51 |
| 13 | 512 | 0.225 | 0.083 | 49 | 60 | 2.77 | 0.62 | 53.13 |
| 14 | 1024 | 0.172 | 0.064 | 54 | 60 | 3.29 | 0.57 | 53.70 |
| 15† | 2048 | 0.118 | 0.051 | 49 | 60 | 4.18 | 0.49 | 54.19 |
| 16 | 4096 | 0.105 | 0.048 | 45 | 60 | 7.41 | 0.78 | 54.97 |
| 17 | 8192 | 0.091 | 0.046 | 45 | 60 | 13.61 | 1.24 | 56.21 |
| 18 | 16,384 | 0.080 | 0.044 | 45 | 60 | 24.91 | 1.99 | 58.20 |
| 19 | 32,768 | 0.072 | 0.044 | 45 | 60 | 49.82 | 3.59 | 61.79 |
| 20 | 65,536 | 0.066 | 0.043 | 45 | 60 | 95.17 | 6.28 | 68.07 |
| 21 | 131,072 | 0.061 | 0.043 | 45 | 60 | 190.34 | 11.61 | 79.68 |
| 22 | 262,144 | 0.056 | 0.043 | 45 | 60 | 380.69 | 21.32 | 101.00 |
| 23 | 524,288 | 0.053 | 0.043 | 45 | 60 | 761.37 | 40.35 | 141.35 |
| 24‡ | $2.31 \times 10^7$ | 0.025 | 0.030 | 45 | 60 | — | 298.13 | 439.48 |

†Terminal bronchioles.

‡Alveoli.

$n$=generation number; $L$=airway segment length; $d$=segment diameter; $\Theta$=branching angle; $\Phi$=gravity angle with 90° corresponding to a horizontal tube; $S$=cross-sectional area; $V$=volume; $\Sigma V$=cumulative volume.

TABLE AIII

Typical Path Lung Model: Human—Right Lower Lobe

| $n$ | Number of tubes | $L$ (cm) | $d$ (cm) | $\Theta$ (°) | $\Phi$ (°) | $S$ ($cm^2$) | $V$ ($cm^3$) | $\Sigma V$ ($cm^3$) |
|---|---|---|---|---|---|---|---|---|
| 1 | 1 | 10.0 | 2.01 | 0 | 0 | 3.17 | 31.73 | 31.73 |
| 2 | 1 | 3.09 | 1.75 | 25 | 25 | 2.41 | 7.43 | 39.16 |
| 3 | 1 | 3.02 | 1.33 | 15 | 5 | 1.39 | 4.20 | 43.36 |
| 4 | 1 | 0.880 | 1.01 | 5 | 5 | 0.80 | 0.71 | 44.06 |
| 5 | 2 | 1.09 | 0.800 | 23 | 28 | 1.01 | 1.10 | 45.16 |
| 6 | 4 | 1.33 | 0.650 | 31 | 36 | 1.33 | 0.86 | 46.02 |
| 7 | 8 | 1.22 | 0.583 | 29 | 34 | 2.14 | 2.61 | 48.63 |
| 8 | 16 | 0.796 | 0.471 | 33 | 30 | 2.79 | 2.22 | 50.85 |
| 9 | 32 | 0.803 | 0.367 | 31 | 27 | 3.39 | 2.72 | 53.57 |
| 10 | 64 | 0.880 | 0.347 | 34 | 35 | 6.05 | 5.33 | 58.89 |
| 11 | 128 | 0.900 | 0.317 | 24 | 38 | 10.10 | 9.09 | 67.98 |
| 12 | 256 | 0.591 | 0.249 | 30 | 44 | 12.47 | 7.37 | 75.35 |
| 13 | 512 | 0.449 | 0.181 | 38 | 39 | 13.17 | 5.92 | 81.27 |
| 14 | 1024 | 0.337 | 0.134 | 51 | 47 | 14.44 | 4.87 | 86.13 |
| 15 | 2048 | 0.257 | 0.101 | 55 | 60 | 16.41 | 4.22 | 90.35 |
| 16 | 4096 | 0.222 | 0.077 | 59 | 60 | 19.07 | 4.23 | 94.58 |
| 17† | 8192 | 0.158 | 0.066 | 56 | 60 | 28.04 | 4.43 | 99.01 |
| 18 | 16,384 | 0.131 | 0.058 | 45 | 60 | 43.29 | 5.67 | 104.68 |
| 19 | 32,768 | 0.110 | 0.054 | 45 | 60 | 75.05 | 8.26 | 112.94 |
| 20 | 65,536 | 0.094 | 0.051 | 45 | 60 | 133.88 | 12.58 | 125.52 |
| 21 | 131,072 | 0.082 | 0.048 | 45 | 60 | 237.18 | 19.45 | 144.97 |
| 22 | 262,144 | 0.072 | 0.046 | 45 | 60 | 435.66 | 31.37 | 176.34 |
| 23 | 524,288 | 0.064 | 0.045 | 45 | 60 | 833.84 | 53.37 | 229.71 |
| 24 | 1,048,576 | 0.058 | 0.044 | 45 | 60 | 1594.39 | 92.47 | 322.18 |
| 25 | 2,097,152 | 0.053 | 0.043 | 45 | 60 | 3045.49 | 161.41 | 483.59 |
| 26‡ | $9.23 \times 10^7$ | 0.025 | 0.030 | 45 | 60 | — | 1191.22 | 1674.82 |

†Terminal bronchioles.

‡Alveoli.

$n$=generation number; $L$=airway segment length; $d$=segment diameter; $\Theta$=branching angle; $\Phi$=gravity angle with 90° corresponding to a horizontal tube; $S$=cross-sectional area; $V$=volume; $\Sigma V$=cumulative volume.

TABLE AIV
Typical Path Lung Model: Human—Upper Lobe

| $n$ | Number of tubes | $L$ (cm) | $d$ (cm) | $\Theta$ (°) | $\Phi$ (°) | $S$ ($cm^2$) | $V$ ($cm^3$) | $\Sigma V$ ($cm^3$) |
|---|---|---|---|---|---|---|---|---|
| 1 | 1 | 10.0 | 2.01 | 0 | 0 | 3.17 | 31.73 | 31.73 |
| 2 | 1 | 5.63 | 1.38 | 40 | 15 | 1.50 | 8.42 | 40.15 |
| 3 | 1 | 1.45 | 1.03 | 35 | 50 | 0.83 | 1.21 | 41.36 |
| 4 | 2 | 1.08 | 0.835 | 30 | 18 | 1.10 | 1.18 | 42.54 |
| 5 | 4 | 1.02 | 0.640 | 21 | 35 | 1.29 | 1.31 | 43.86 |
| 6 | 8 | 1.09 | 0.535 | 15 | 33 | 1.80 | 1.96 | 45.82 |
| 7 | 16 | 1.02 | 0.426 | 25 | 45 | 2.28 | 2.33 | 48.14 |
| 8 | 32 | 0.751 | 0.341 | 28 | 37 | 2.92 | 2.19 | 50.34 |
| 9 | 64 | 0.832 | 0.307 | 28 | 42 | 4.74 | 3.94 | 54.28 |
| 10 | 128 | 0.555 | 0.234 | 25 | 49 | 5.50 | 3.06 | 57.33 |
| 11 | 256 | 0.482 | 0.178 | 34 | 43 | 6.37 | 3.07 | 60.40 |
| 12 | 512 | 0.388 | 0.135 | 34 | 44 | 7.33 | 2.84 | 63.25 |
| 13 | 1024 | 0.343 | 0.100 | 41 | 60 | 8.04 | 2.76 | 66.01 |
| 14 | 2048 | 0.267 | 0.078 | 47 | 60 | 9.79 | 2.61 | 68.62 |
| 15† | 4096 | 0.215 | 0.061 | 55 | 60 | 11.97 | 2.57 | 71.19 |
| 16 | 8192 | 0.175 | 0.055 | 45 | 60 | 19.46 | 3.41 | 74.60 |
| 17 | 16,384 | 0.144 | 0.051 | 45 | 60 | 33.47 | 4.82 | 79.42 |
| 18 | 32,768 | 0.118 | 0.048 | 45 | 60 | 59.30 | 7.00 | 86.41 |
| 19 | 65,536 | 0.098 | 0.047 | 45 | 60 | 113.70 | 11.14 | 97.56 |
| 20 | 131,072 | 0.082 | 0.045 | 45 | 60 | 208.46 | 17.09 | 114.65 |
| 21 | 262,144 | 0.071 | 0.044 | 45 | 60 | 398.60 | 28.30 | 141.95 |
| 22 | 524,288 | 0.060 | 0.044 | 45 | 60 | 797.20 | 47.83 | 190.78 |
| 23 | 1,048,576 | 0.053 | 0.043 | 45 | 60 | 1522.74 | 80.71 | 271.49 |
| 24‡ | $4.62 \times 10^7$ | 0.025 | 0.030 | 45 | 60 | — | 596.26 | 867.75 |

†Terminal bronchioles.
‡Alveoli.
$n$ = generation number; $L$ = airway segment length; $d$ = segment diameter; $\Theta$ = branching angle; $\Phi$ = gravity angle with 90° corresponding to a horizontal tube; $S$ = cross-sectional area; $V$ = volume; $\Sigma V$ = cumulative volume.

TABLE AV

Typical Path Lung Model: Human—Left Lower Lobe

| $n$ | Number of tubes | $L$ (cm) | $d$ (cm) | $\Theta$ (°) | $\Phi$ (°) | $S$ ($cm^2$) | $V$ ($cm^3$) | $\Sigma V$ ($cm^3$) |
|---|---|---|---|---|---|---|---|---|
| 1 | 1 | 10.0 | 2.01 | 0 | 0 | 3.17 | 31.73 | 31.73 |
| 2 | 1 | 5.63 | 1.38 | 40 | 15 | 1.50 | 8.42 | 40.15 |
| 3 | 1 | 1.42 | 1.15 | 25 | 10 | 1.04 | 1.47 | 41.63 |
| 4 | 2 | 1.33 | 0.905 | 48 | 55 | 1.29 | 1.71 | 43.34 |
| 5 | 4 | 1.13 | 0.680 | 25 | 48 | 1.45 | 1.64 | 44.98 |
| 6 | 8 | 0.891 | 0.559 | 31 | 41 | 1.96 | 1.75 | 46.73 |
| 7 | 16 | 1.02 | 0.454 | 22 | 39 | 2.59 | 2.64 | 49.37 |
| 8 | 32 | 0.836 | 0.365 | 27 | 37 | 3.35 | 2.80 | 52.17 |
| 9 | 64 | 0.778 | 0.316 | 27 | 36 | 5.02 | 3.91 | 56.07 |
| 10 | 128 | 0.771 | 0.298 | 28 | 36 | 8.93 | 6.88 | 62.96 |
| 11 | 256 | 0.611 | 0.286 | 31 | 46 | 16.45 | 10.05 | 73.01 |
| 12 | 512 | 0.544 | 0.211 | 40 | 45 | 17.90 | 9.74 | 82.75 |
| 13 | 1024 | 0.431 | 0.146 | 46 | 48 | 17.14 | 7.39 | 90.13 |
| 14 | 2048 | 0.302 | 0.102 | 50 | 60 | 16.73 | 5.05 | 95.19 |
| 15 | 4096 | 0.224 | 0.076 | 52 | 60 | 18.58 | 4.16 | 99.35 |
| 16† | 8192 | 0.188 | 0.061 | 54 | 60 | 23.94 | 4.50 | 103.85 |
| 17 | 16,384 | 0.152 | 0.055 | 45 | 60 | 38.93 | 5.92 | 109.77 |
| 18 | 32,768 | 0.124 | 0.051 | 45 | 60 | 66.94 | 8.30 | 118.07 |
| 19 | 65,536 | 0.103 | 0.049 | 45 | 60 | 123.58 | 12.73 | 130.80 |
| 20 | 131,072 | 0.087 | 0.047 | 45 | 60 | 227.40 | 19.78 | 150.58 |
| 21 | 262,144 | 0.076 | 0.046 | 45 | 60 | 435.66 | 33.11 | 183.69 |
| 22 | 524,288 | 0.066 | 0.045 | 45 | 60 | 833.84 | 55.03 | 238.73 |
| 23 | 1,048,576 | 0.059 | 0.044 | 45 | 60 | 1594.39 | 94.07 | 332.79 |
| 24 | 2,097,152 | 0.053 | 0.043 | 45 | 60 | 3045.49 | 161.41 | 494.21 |
| 25‡ | $9.23 \times 10^7$ | 0.025 | 0.030 | 45 | 60 | — | 1191.22 | 1685.43 |

†Terminal bronchioles.

‡Alveoli.

$n$ = generation number; $L$ = airway segment length; $d$ = segment diameter; $\Theta$ = branching angle; $\Phi$ = gravity angle with 90° corresponding to a horizontal tube; $S$ = cross-sectional area; $V$ = volume; $\Sigma V$ = cumulative volume.

TABLE AVI
Comparison of Lobar Lung Volume and Anatomical Death Space, in $cm^3$, for Human Lung Models at Total Lung Capacity

| | Anatomical dead space | | | Lung volume | |
|---|---|---|---|---|---|
| Lobe | Lobar model | Lung cast† | Whole lung model | Lobar model | Whole lung model |
| Right upper | 25.63 | — | — | 803.55 | — |
| Right middle | 10.83 | — | — | 396.12 | — |
| Right lower | 55.65 | — | — | 1631.46 | — |
| Left upper | 31.04 | — | — | 827.60 | — |
| Left lower | 63.70 | — | — | 1645.28 | — |
| Others (common stems) | 51.78 | — | — | 51.78 | — |
| Whole lung | 238.63 | 210 | 227.21 | 5355.79 | 5563.88 |

†Gravimetric technique.

TABLE AVII
Relative Lobar Sizes in the Human Lung†

| Lobe | Model | Cast‡ | Horsfield§ | Baker¶ |
|---|---|---|---|---|
| Right upper | 15.4 | 17.8 | 19 | — |
| Right middle | 7.7 | 7.1 | 10 | — |
| Right lower | 30.8 | 28.4 | 26 | — |
| Left upper | 15.4 | 17.6 | 19 | — |
| Left lower | 30.8 | 29.2 | 26 | — |
| Right:left | 54:46 | 53:47 | 55:45 | 55:45 |

†In % of total lung.
‡Estimated from number of 3 mm segments.
§Horsfield, K. *et al., J. Appl. Physiol.* **31,** 207–217, 1971.
¶Baker, R. D., *Postmortem Examination,* Saunders: Philadelphia, 1967, p. 174.

## LITERATURE

Altshuler, B., E. D. Palmes and N. Nelson. 1967. "Regional Aerosol Deposition in the Human Respiratory Tract." In: *Inhaled Particles and Vapours* II, pp. 323–335, edited by C. N. Davies. New York: Pergamon Press.

Beeckmans, J. M. 1965a. "The Deposition of Aerosols in the Respiratory Tract: I. Mathematical Analysis and Comparison with Experimental Data." *Can. J. Physiol. Pharmacol.* **43,** 157–172.

Beeckmans, J. M. 1965b. "Correction Factor for Size-selective Sampling Results, Based on a New Computed Alveolar Deposition Curve." *Ann. Occup. Hyg.* **8,** 221–231.

Davies, C. N. 1961. "A Formalized Anatomy of the Human Respiratory Tract." In: *Inhaled Particles and Vapours,* pp. 82–87, edited by C. N. Davies. New York: Pergamon Press.

Davies, C. N. 1973. "The Deposition of Aerosol in the Human Lung." In: *Aerosole in Physik, Medizin und Technik*, pp. 90–99. Bad Soden, W. Germany: Gesellschaft fur Aerosolforschung.

Findeisen, W. 1935. "Uber das Absetzen Kleiner, in der Luft Suspendierter Teilchen in der Menschlichen Lunge bei der Atmung." *Pfluegers Arch. Ges. Physiol.* **236,** 367–379.

Giacomelli-Maltoni, G., C. Melandri, V. Prodi and G. Tarroni. 1972. "Deposition Efficiency of Monodisperse Particles in Human Respiratory Tract." *Am. Ind. Hyg. Assoc. J.* **33**(9), 603–610.

Heyder, J., L. Armbruster, J. Gebhart, E. Grein and W. Stahlhofen. 1975. "Total Deposition of Aerosol Particles in the Human Respiratory Tract for Nose and Mouth Breathing." *J. Aerosol Sci.* **6,** 311–328.

Horsfield, K., G. Dart, D. E. Olson, G. F. Filley and G. Cumming. 1971. "Models of the Human Bronchial Tree." *J. Appl. Physiol.* **31**(2), 207–217.

International Commision on Radiological Protection (ICRP). 1974. *Report of the Task Group on Reference Man. ICRP Publication* 23. Oxford: Pergamon Press.

Landahl, H. D. 1950. "On the Removal of Air-borne Droplets by the Human Respiratory Tract: I. The Lung." *Bull. Math. Biophys.* **12,** 43–56.

Landahl, H. D., T. N. Tracewell and W. H. Lassen. 1951. "On the Retention of Air-borne Particulates in the Human Lung." *A.M.A. Arch. Ind. Hyg. Occup. Med.* **3,** 359–366.

Lever, J. 1973. Cited by C. N. Davies.

Lippmann, M. 1977. Regional Deposition of Particles in the Human Respiratory Tract. In: *Handbook of Physiology*, Section 9: *Reactions to Environmental Agents*, pp. 213–232, edited by D. H. K. Lee. Bethesda, Md.: Am. Physiology Soc.

Mercer, T. T. 1975. "The Deposition Model of the Task Group on Lung Dynamics: A Comparison with Recent Experimental Data." *Hlth Phys.* **29,** 673–680.

Olson, D. E., G. A. Dart and G. F. Filley. 1970. "Pressure Drop and Fluid Flow Regime of Air Inspired into the Human Lung." *J. Appl. Physiol.* **28**(4), 482–494.

Phalen, R. F., H. C. Yeh, O. G. Raabe and D. J. Velasquez. 1973. "Casting the Lungs *in situ*." *Anat. Rec.* **177,** 255–263.

Phalen, R. F., H. C. Yeh, G. M. Schum and O. G. Raabe. 1978. "Application of an Idealized Model to Morphometry of the Mammalian Tracheobronchial Tree." *Anat. Rec.* **190**(2), 167–176.

Schum, G. M. and H. C. Yeh. 1979. "Theoretical Evaluation of Aerosol Deposition in Anatomical Models of Mammalian Lung Airways." *Bull. Math. Biol.* **42,** 1–15.

Task Group on Lung Dynamics. 1966. "Deposition and Retention Models for Internal Dosimetry of the Human Respiratory Tract." *Hlth Phys.* **12,** 173–207.

Taulbee, D. B. and C. P. Yu. 1975. "A Theory of Aerosol Deposition in the Human Respiratory Tract." *J. Appl. Physiol.* **38**(1), 77–85.

Weibel, E. R. 1963. *Morphometry of the Human Lung.* New York: Academic Press.

Yeh, H. C., A. J. Hulbert, R. F. Phalen, D. J. Velasquez and T. D. Harris. 1975. "A Stereoradiographic Technique and Its Application to the Evaluation of Lung Casts." *Invest. Radiol.* **10,** 351–357.

Yeh, H. C., R. F. Phalen and O. G. Raabe. 1976. "Factors Influencing the Deposition of Inhaled Particles." *Environ. Hlth Perspect.* **15,** 147–156.

Yeh, H. C., G. M. Schum and M. T. Duggan. 1979. "Anatomical Models of the Tracheobronchial and Pulmonary Regions of the Rat." *Anat. Rev.* **195,** 483–492.

Yeh, H. C. 1979, "Modeling of Biological Tree Structures," *Bull. Math. Biol.* 41, 893–898.